Received: 7 March 2022 | Accepted: 3 June 2022

DOI: 10.1111/1751-7915.14102

RESEARCH ARTICLE

microbial biotechnology Open Access

Modulation of yeast Erg1 expression and terbinafine susceptibility by iron bioavailability

Tania Jordá[1] | **Ana Martínez-Martín**[1] | **María Teresa Martínez-Pastor**[2] | **Sergi Puig**[1]

[1]Departamento de Biotecnología, Instituto de Agroquímica y Tecnología de Alimentos (IATA), Consejo Superior de Investigaciones Científicas (CSIC), Paterna, Valencia, Spain

[2]Departamento de Bioquímica y Biología Molecular, Universitat de València, Burjassot, Valencia, Spain

Correspondence
Sergi Puig, Dept. Biotecnología, IATA-CSIC, Catedrático Agustín Escardino 7, Paterna, Valencia, Spain.
Email: spuig@iata.csic.es

Funding information
This research was supported by grant PID2020-116940RB-I00 funded by MCIN/AEI/10.13039/501100011033 and predoctoral fellowship ACIF/2019/214 funded by 'Generalitat Valenciana'. We also acknowledge support of the publication fee by the CSIC Open Access Publication Support Initiative through its Unit of Information Resources for Research (URICI).

Abstract

Ergosterol is a specific sterol component of yeast and fungal membranes. Its biosynthesis is one of the most effective targets for antifungal treatments. However, the emergent resistance to multiple sterol-based antifungal drugs emphasizes the need for new therapeutic approaches. The allylamine terbinafine, which selectively inhibits squalene epoxidase Erg1 within the ergosterol biosynthetic pathway, is mainly used to treat dermatomycoses, whereas its effectiveness in other fungal infections is limited. Given that ergosterol biosynthesis depends on iron as an essential cofactor, in this report, we used the yeast *Saccharomyces cerevisiae* to investigate how iron bioavailability influences Erg1 expression and terbinafine susceptibility. We observed that both chemical and genetic depletion of iron decrease *ERG1* expression, leading to an increase in terbinafine susceptibility. Deletion of either *ROX1* transcriptional repressor or *CTH1* and *CTH2* post-transcriptional repressors of *ERG1* expression led to an increase in Erg1 protein levels and terbinafine resistance. On the contrary, overexpression of *CTH2* led to the opposite effect, lowering Erg1 levels and increasing terbinafine susceptibility. Although strain-specific particularities exist, opportunistic pathogenic strains of *S. cerevisiae* displayed a response similar to the laboratory strain. These data indicate that iron bioavailability and particular regulatory factors could be used to modulate susceptibility to terbinafine.

INTRODUCTION

The major yeast and fungal-specific sterol, ergosterol, is responsible for maintaining cell integrity and function of biological membranes. Therefore, ergosterol biosynthesis is one of the most clinically effective targets of antifungal drugs. Azoles, which inhibit lanosterol 14α-demethylase, have been very successful in clinical and agricultural applications. However, the plastic genome and rapid reproduction of fungi frequently lead to the generation of pathogens resistant to the most common chemicals used in medicine and agriculture, including azoles (Fisher et al., 2018). The relative high toxicity and emergent resistance to azoles emphasizes the need for new therapeutic approaches and additional drugs (Monk et al., 2020). Allylamines selectively inhibit squalene epoxidase (also known as squalene monooxygenase [SM]), which catalyses the rate-limiting step of squalene epoxidation to 2, 3-oxidosqualene within the ergosterol biosynthesis pathway, leading to the

accumulation of squalene and the depletion of ergosterol (Ryder, 1992). Squalene epoxidase is encoded in *Saccharomyces cerevisiae* by the essential *ERG1* gene. The allylamine terbinafine is the first-line drug for dermatomycoses treatment, one of the most common fungal infections (Gnat et al., 2020). Conversely to dermatophytes, yeasts such as *Candida albicans* and moulds such as *Aspergillus fumigatus* exhibit reduced terbinafine susceptibility (Ryder, 1992; Ryder et al., 1998). Moreover, terbinafine resistance in pathogenic fungi is increasing and has been linked to non-synonymous point mutations in *ERG1* (Sagatova, 2021). Most of these mutations seem to change the size of the hydrophobic side-chains on the Erg1 inhibitor-binding pocket, which overlaps with the squalene binding site, altering hydrophobic interactions with the drug (Sagatova, 2021). Improving the efficacy of terbinafine in yeasts, fungi and moulds would have significant benefits in medicine and agriculture. Furthermore, its combination with drugs with different modes of action would increase efficacy and reduce therapeutic doses, while slowing down the emergence of resistance. On the other hand, the human Erg1 homologue also catalyses the rate-limiting step of squalene epoxidation within human cholesterol biosynthesis, and the use terbinafine (which binds to human SM with lower affinity) and other SM inhibitors has been considered for the treatment of hypercholesterolemia and certain cancer types (Chua et al., 2020).

Iron is a vital micronutrient for all eukaryotic organisms, its depletion being an important limitation for microbial growth and the virulence of pathogens (Martinez-Pastor & Puig, 2020). Hence, hosts restrict iron bioavailability upon fungal infections and the treatment with iron chelators is used against multiple pathogens (Hosogaya et al., 2013; Lai et al., 2016). In addition to its indispensable role in respiration and DNA and protein synthesis, iron is an essential cofactor in four enzymatic steps of the ergosterol biosynthesis pathway (Jorda & Puig, 2020). Thus, iron deficiency reduces the metabolic flux through the ergosterol pathway and leads to the accumulation of the initial substrates, squalene and lanosterol (Jorda et al., 2021; Shakoury-Elizeh et al., 2010).

Saccharomyces cerevisiae is widely recognized as a model organism to study fungal iron and lipid metabolisms, and an excellent system to explore how iron influences antifungal drugs based on ergosterol biosynthesis targeting (Demuyser & Van Dijck, 2019; Martinez-Pastor & Puig, 2020; Singh, 2016). *S. cerevisiae* has also been extensively used as a safe microorganism for food biotechnological and nutritional purposes, being in turn associated with biotherapeutic and probiotic properties (Llopis et al., 2014). However, over the past 25 years, the incidence of invasive *S. cerevisiae* infections is increasing, especially in immunocompromised patients or with breached epithelial barriers (Perez-Torrado & Querol, 2015; Wombwell et al., 2021). Virulence phenotypic traits of several *S. cerevisiae* strains with clinical origin or used as dietary supplements have been contrasted both in vitro and in vivo with murine models (Clemons et al., 1994; de Llanos et al., 2006; de Llanos et al., 2011; Llopis et al., 2014; Yañez et al., 2009). The symptoms of these infections are indistinguishable from invasive candidiasis.

In this report, we investigate how iron bioavailability influences *ERG1* expression and terbinafine susceptibility in laboratory and clinically relevant *S. cerevisiae* strains. We identify various factors that regulate *ERG1* expression during iron depletion. Modulating these regulatory factors and fungal iron availability could be explored to develop novel strategies to improve terbinafine treatments.

EXPERIMENTAL PROCEDURES

Yeast strains, growth conditions and plasmids

The *S. cerevisiae* strains used in this report are listed in Table S1. Yeast *rox1Δ* and *cth1Δcth2Δ* mutants were constructed in the FY2609 background using the genomic DNA of the corresponding mutants in the BY4741 background as a template to generate integrative cassettes for disruption.

Prior to experiments, yeast precultures were cultivated overnight at 30°C in liquid synthetic complete (SC) medium [0.17% yeast nitrogen base without amino acids and without ammonium sulfate (Pronadisa), 0.5% ammonium sulfate (Panreac), 2% glucose (Panreac) and 2 g/L Kaiser drop-out (Formedium)] lacking specific requirements when necessary. For RNA and protein analyses, cells were reinoculated in 50 ml of SC and incubated for 15 h at 190 rpm to early exponential phase. At that moment, 100 μM of the Fe^{2+}-specific chelator bathophenanthroline disulfonic acid disodium (BPS) (Sigma) or 300 μM ferrous ammonium sulfate (FAS) (Sigma) was added to create iron deficiency or iron-enriched media, respectively. In Figure 5, BY4741 *cth1Δcth2Δ* cells transformed with the centromeric plasmids pRS416-CTH2 (*CTH2*) or p416TEFCTH2 (P_{TEF}-*CTH2*) (Puig et al., 2005; Puig et al., 2008) were grown overnight, reinoculated at an OD_{600} of 0.2 and then incubated for 6 h to exponential phase in SC-ura or SC-ura with 100 μM BPS.

To construct the p413TEF-ERG1 (P_{TEF}-*ERG1*) plasmid, the coding sequence of *ERG1* gene was amplified with ERG1-Xba1-F and ERG1-Sal1-R oligonucleotides (Table S2), and the PCR product was cloned into the p413TEF plasmid using the restriction enzymes XbaI (Roche) and SalI (Roche). PCR amplifications were performed with Phusion polymerase (Finnzymes) and the cloned insert was sequenced. NZY5α competent

Escherichia coli cells (NYZtech) were used to isolate and propagate the plasmid.

RNA analyses

Total RNA extraction and cellular mRNA levels were determined by RT-qPCR as previously described (Sanvisens et al., 2014). Primers used for RT-qPCR are listed in Table S2.

Protein analyses

Total protein isolations were carried out with the alkali method as previously described (Kushnirov, 2000), and proteins were resolved in SDS-PAGE gels were transferred to nitrocellulose membranes. The primary antibodies used were anti-Erg1 and anti-Pgk1 (22C5D8; Invitrogen). Immunoblots were developed with the corresponding horseradish peroxidase-labelled secondary antibodies and the ECL Select Western blotting detection kit (GE Healthcare Life Sciences). Images were obtained with an Amersham ImageQuant 800 biomolecular imager.

Polyribosome profile analysis

Polyribosome gradient profiles were carried out as previously described (Ramos-Alonso et al., 2018). Specific mRNAs were analysed by RT-qPCR and represented as a percentage of total. All the values were normalized with spiked-in mRNA levels of *Bacillus subtilis phe*.

Drug susceptibility testing

In vitro susceptibility testing of terbinafine was performed according to the Clinical and Laboratory Standards Institute document M38-A2 ([CLSI], 2008). However, instead of visual reading to end-point determination, we used a spectrophotometric method, monitoring growth at 600 nm in a SpectroStar Nano 96-well plate reader (BMGLabtech) every 0.5 h over 72 h after a pre-shaking of 20 s. The incubation temperature was 28°C, except for the experiments with pathogenic yeast strains that were carried out at 37°C. Each kinetics was made in triplicate or quadruplicate. To estimate the IC80 parameter (concentration that inhibits growth by 80%), we compared the area under the curve of OD_{600} versus time at 48 h of a positive control (without terbinafine) with the areas of the tests (with increasing concentration of terbinafine) as previously described in *S. cerevisiae* (Arroyo-Lopez et al., 2010). According to the equation used to determine the MIC parameter (Arroyo-Lopez et al., 2010), we estimated the IC50 and IC80 parameters as:

$$IC50 = 10^{\left[M+\left(\frac{1}{B}\right)*\log(\log 2)\right]} \quad IC80 = 10^{\left[M+\left(\frac{1}{B}\right)*\log(\log 5)\right]}$$

where M is the $\log_{10}$ of terbinafine concentration of the inflexion point and B is a slope parameter.

Terbinafine (Sigma-Aldrich) was obtained in the powder form and drug stock solution was prepared in methanol to the final concentration of 10 mg/ml. The drug was analysed in the range from 3.12 to 400 μg/ml, and 3.12–800 μg/ml in the case P_{TEF}-*ERG1* strain. The final methanol concentration in the wells was below 6% and had no effect on growth.

Statistical analyses

The statistical analysis of the relative gene expression was performed by the pair wise fixed reallocation randomization test (Pfaffl et al., 2002) using the InfoStat software. For the remaining parameters, statistical significance was evaluated with tailed t-Student's test. Different letters above the bars represent significant differences among groups (p-value < 0.05).

RESULTS

Yeast Erg1 protein levels decrease in response to iron deficiency

Consistent with the ergosterol biosynthesis pathway being dependent on iron in four enzymatic steps, genome-wide expression studies have shown that the transcript levels of multiple *ERG* genes are altered in response to iron deficiency (Hausmann et al., 2008; Puig et al., 2005; Romero et al., 2019). To ascertain how iron bioavailability affects the mRNA levels of yeast squalene epoxidase *ERG1* gene, we cultivated wild-type (WT) cells in a synthetic complete (SC) medium containing 100 μM of the Fe^{2+}-specific chelator bathophenanthroline disulfonic acid (BPS). Then, we analysed *ERG1* transcript levels by RT-qPCR at 3 and 7 h after the addition of BPS. We observed that *ERG1* transcript abundance decreased at 3 h of iron depletion, but partially recovered its initial mRNA levels after 7 h of scarcity (Figure 1A). To certify that this observation was due to iron depletion but not to a side-effect of BPS, we used the yeast strain *fet3Δfet4Δ*, which is genetically deficient in iron uptake due to the lack of both high- and low-affinity iron acquisition systems at the cell surface. We observed that *fet3Δfet4Δ* cells displayed lower *ERG1* mRNA levels than WT cells under normal SC conditions (Figure 1A). Importantly, addition of iron to the SC medium (300 μM ferrous ammonium sulfate, FAS) increased *fet3Δfet4Δ ERG1* transcript

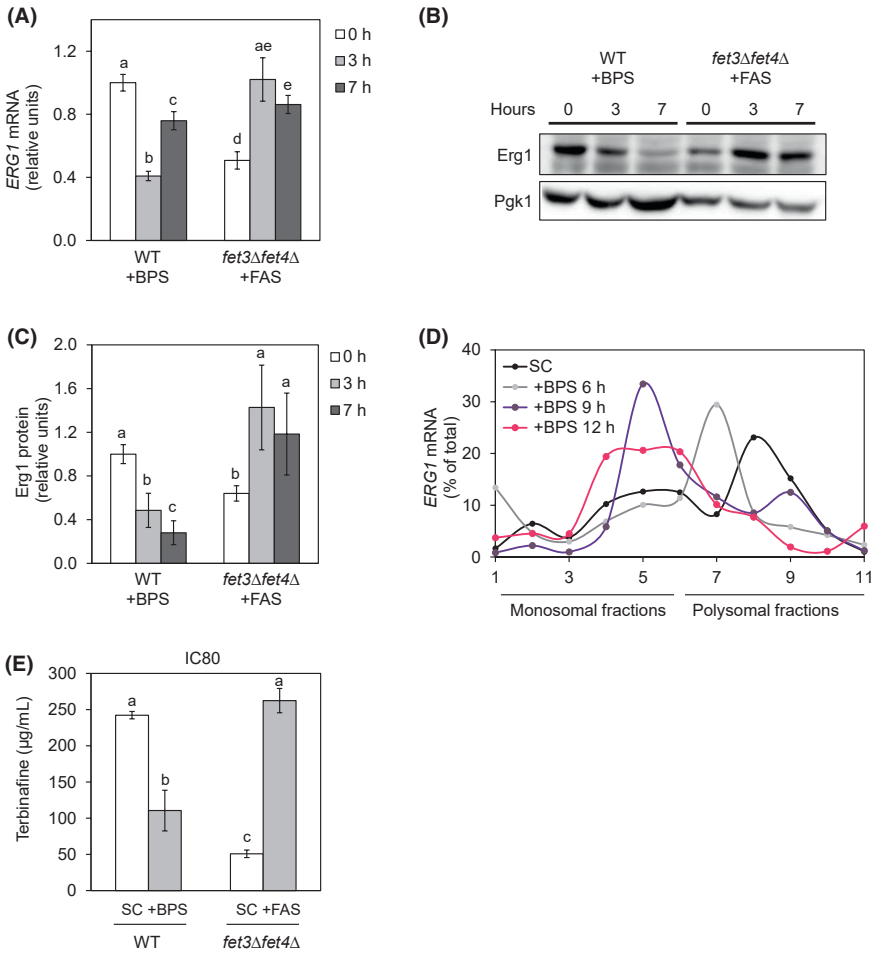

FIGURE 1 Iron deficiency affects *ERG1* expression and terbinafine susceptibility. (A–C) Wild-type (WT, BY4741) and *fet3Δfet4Δ* strains were cultivated overnight in SC medium at 30°C to exponential phase. Then, an aliquot was extracted (time 0 h, SC) and 100 µM BPS or 300 µM FAS was added to wild-type or *fet3Δfet4Δ* cells, respectively. Cells were cultured 7 additional hours, and aliquots were isolated at 3 and 7 h. (A) Total RNA was extracted and *ERG1* mRNA levels normalized to *ACT1* mRNA were determined by RT-qPCR as described in Materials and Methods. Data show the average and standard deviation (*SD*) of three biologically independent experiments relative to WT strain grown in SC. (B) The protein levels of Erg1 and the loading control Pgk1 were analysed by Western blot with anti-Erg1 and anti-Pgk1 antibodies, respectively. (C) Quantification of Erg1 protein levels normalized to Pgk1. Data show the average and SD of two biological replicates relative to WT strain grown in SC. (D) The translation of *ERG1* gene decreases in iron deficiency. The RNA in individual polysomal fractions was extracted and *ERG1* mRNA levels, normalized to *phe* mRNA, were analysed by RT-qPCR. Monosomal and polysomal fractions are indicated. (E) Iron-deprived cells are more susceptible to terbinafine. WT and *fet3Δfet4Δ* cells were cultivated at 28°C as in panel A and the terbinafine concentrations that inhibited 80% of growth (IC80) were determined as described in Materials and Methods. A drug range between 3.12 and 400 µg/ml was used. Data show the average and SD of IC80 values of three biological samples. Different letters above the bars represent statistically significant differences (p-value < 0.05).

levels to reach those of a WT strain under normal conditions (Figure 1A). As expected, both BPS addition and *FET3*/*FET4* deletion limited growth, which was recovered after supplementation with FAS (Figure URE S1A). Then, we used a specific antibody to determine Erg1 protein levels under the same growth conditions. Similar to mRNA data, we observed that both BPS and deletion of *FET3*/*FET4* led to a decrease in Erg1 protein abundance (Figure 1B, C). Addition of iron to *fet3Δfet4Δ* cells also increased Erg1 levels (Figure 1B, C). However, prolonged iron depletion (7 h in BPS) did not recover Erg1 protein levels of WT cells as observed for mRNA data, but showed a further decrease in Erg1 abundance (Figure 1B, C). These results indicate that Erg1 protein concentration is mainly downregulated during the progress of iron scarcity.

To investigate the lack of correspondence between *ERG1* mRNA and protein levels after 7 h of iron depletion, we determined the association of *ERG1* transcript to ribosomes. We have previously observed that iron deficiency causes a bulk repression of translation that could be responsible for the decrease in Erg1 protein abundance (Romero et al., 2020). Thus, we performed ribosome profiles under both iron-sufficient and iron-deficient conditions and isolated RNA from different fractions. We observed that *ERG1* mRNA decreased its association to polysomes and increased its abundance in monosomal fractions as iron deficiency progressed

(Figure 1D). These results suggest that the drop in Erg1 protein levels that occurs during the progress of iron starvation is due to a global drop in translation.

Yeast susceptibility to terbinafine increases in iron-deficient conditions

Erg1 is the main target of the antifungal drug terbinafine (Ryder, 1992). Therefore, we evaluated the impact of altering Erg1 levels on terbinafine resistance by modulating intracellular iron. Given that iron deficiency leads to a decrease in Erg1 protein abundance, we hypothesized that iron depletion would increase the sensitivity of yeast cells to terbinafine. Thus, we assayed terbinafine susceptibility of *S. cerevisiae* WT cells in iron-sufficient (SC) and iron-deficient (+BPS) media and *fet3Δfet4Δ* mutant in iron-sufficient (SC) and iron-replete (+FAS) conditions by determining the antifungal concentration that inhibits 80% of growth (IC80, see Material and Methods for details). In accordance with our hypothesis, iron depletion by either chemical chelation or genetic downregulation of iron uptake made cells more susceptible to terbinafine (lower IC80), while iron supplementation increased the resistance of *fet3Δfet4Δ* cells to terbinafine (higher IC80) (Figure 1E, S1B). These results are consistent with the changes in Erg1 expression produced by iron availability (Figure 1B, C).

Overexpression of *ERG1* increases resistance to terbinafine

To ascertain whether the reason for the increased susceptibility of iron-deficient cells to terbinafine were changes in Erg1 protein levels, we overexpressed *ERG1* under the control of the constitutive *TEF2* promoter (P_{TEF}-*ERG1*) and determined both *ERG1* levels and terbinafine resistance. The successful overexpression of *ERG1* was confirmed using both RT-qPCR and Western blot (Figure 2A, B), while potential toxic effects on cell growth were ruled out (Figure S2A). Under both conditions of iron-sufficiency and iron-depletion, *ERG1* overexpression increased terbinafine resistance, as it resulted in higher IC80 values (Figure 2C, S2B).

Previous studies have described that terbinafine treatment causes an increase of *ERG1* expression (Leber et al., 2001). Therefore, we evaluated the joint effect of iron deficiency and terbinafine treatment on the levels of *ERG1* mRNA and protein. Results in iron-sufficient conditions showed that Erg1 protein levels were relatively constant, while the levels of *ERG1* mRNA slightly decreased with time (Figure 3, SC). As previously showed (Figure 1), both *ERG1* mRNA and protein levels decreased upon iron limitation achieved by addition of 100 μM BPS (Figure 3, +BPS). As previously reported (Leber et al., 2001), terbinafine treatment

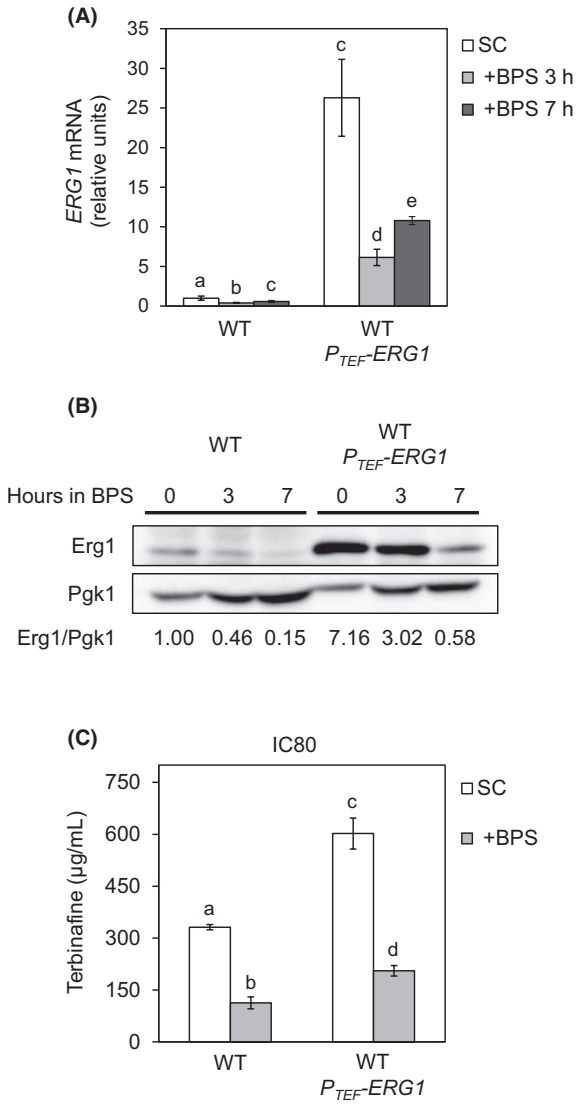

FIGURE 2 *ERG1* overexpression decreases terbinafine susceptibility. (A) and (B) BY4741 yeast cells transformed with the p413TEF empty vector (WT) or the p413TEF-ERG1 plasmid (WT P_{TEF}-*ERG1*) were cultivated in SC-his to exponential phase and aliquots were isolated after the addition of 100 μM BPS. (A) *ERG1* mRNA levels normalized to *ACT1* mRNA were represented in relation to WT strain in SC. Data show the average and SD of three biologically independent experiments relative to WT strain grown in SC. (B) Erg1 and Pgk1 protein levels analysed by Western blot as described in Materials and Methods. Numbers indicate Erg1/Pgk1 changes (n-fold) relative to WT strain in SC of that biological replica. (C) Terbinafine susceptibility decreases with increasing *ERG1* expression even in iron-depleted medium. A terbinafine range of 3.12 to 800 μg/ml was tested at 28°C against WT and WT P_{TEF}-*ERG1* in media without (SC) or with 100 μM BPS (+BPS). Data show the average and SD of IC80 values of four biological samples. Different letters above the bars represent statistically significant differences (p-value < 0.05).

(30 μg/ml) increased the levels of *ERG1* mRNA and protein (Figure 3, +TER). Importantly, the increase in Erg1 abundance caused by terbinafine addition was hampered by chelating iron (Figure 3, +BPS + TER), although the levels of *ERG1* mRNA and protein remained

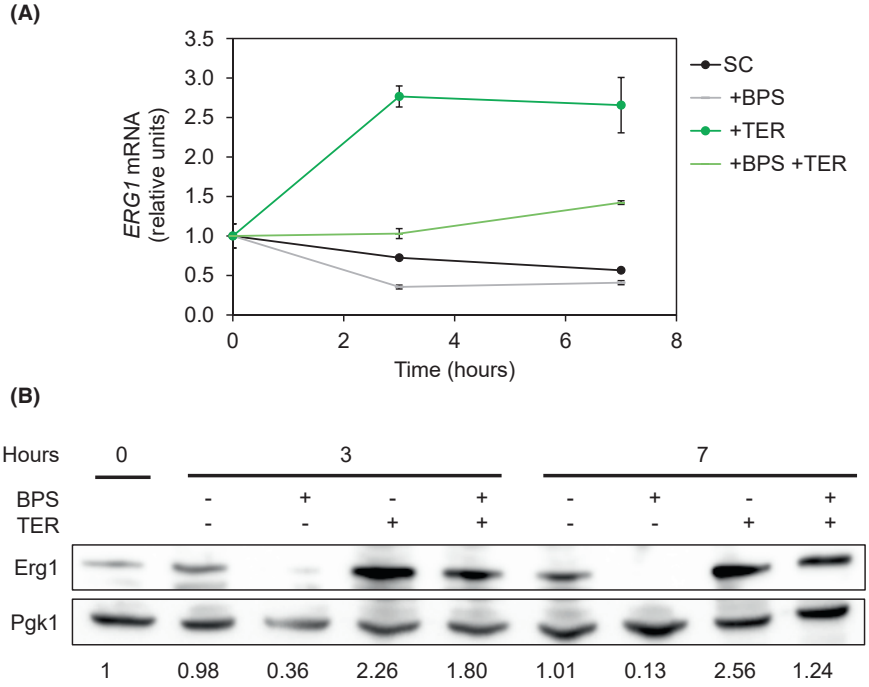

FIGURE 3 Iron deficiency down-regulates *ERG1* expression in terbinafine-treated cells. The BY4741 yeast was growth in SC to exponential phase (time 0) and then nothing (SC), 100 μM BPS (+BPS), 30 μg/ml terbinafine (+TER), or both compounds (+BPS + TER) were added to the medium. Aliquots were isolated for further analysis after 3 and 7 h. (A) *ERG1/ACT1* mRNA levels represented in relation to time 0 in SC are shown as the average of three biological replicates. (B) Western blot image of Erg1 and Pgk1 protein levels of a representative experiment of two biological samples. Numbers indicate Erg1/Pgk1 changes (n-fold) relative to WT strain in SC of that biological replicate.

higher than in strains grown in SC medium. In any case, we can conclude that iron depletion downregulates Erg1 abundance even in the presence of terbinafine, contributing to its susceptibility. We also studied the expression pattern of *PRD5*, which encodes for a plasma membrane ATP-binding cassette multidrug transporter that could be implicated in terbinafine resistance, upon treatment with BPS and terbinafine. We observed that *PDR5* mRNA levels decreased during growth, but no statistical differences were observed among the different treatments (Figure S3).

Rox1 modulates *ERG1* expression and terbinafine susceptibility under iron deficiency

Previous studies in *S. cerevisiae* have reported that deletion of the heme-dependent repressor *ROX1* results in increased *ERG1* mRNA levels and terbinafine resistance (Henry et al., 2002). Thus, we tested whether *ROX1* deletion upregulated *ERG1* expression under iron-depleted conditions. Addition of BPS limited the growth of both WT and *rox1Δ* cells (Figure S4A). We observed that *ERG1* mRNA and protein levels increased in *rox1Δ* mutant under both iron-sufficient and iron-deficient growth conditions (Figure 4A–C). In accordance with Erg1 protein levels, *rox1Δ* cells displayed an increased resistance to terbinafine under both iron replete and iron-depleted conditions (Figure 4D, S4B). These results indicate that Rox1 is a determinant factor of *ERG1* expression and terbinafine susceptibility under iron deficiency.

The iron-regulated Cth1 and Cth2 mRNA-binding proteins modulate *ERG1* expression and terbinafine susceptibility

Previous genome-wide studies suggested that *ERG1* mRNA, which contains putative AREs within its 3'UTR, increased its abundance in iron-deficient cells lacking the RNA-binding proteins Cth1 and Cth2 (Puig et al., 2005; Puig et al., 2008). Cth2 and its homologous Cth1 cooperate in the metabolic adaptation to iron deficiency via targeted ARE-containing mRNAs degradation and translation inhibition (Pedro-Segura et al., 2008; Puig et al., 2005; Puig et al., 2008; Ramos-Alonso et al., 2018). We checked whether the deletion of *CTH1* and *CTH2* increased *ERG1* mRNA levels. We observed that indeed *cth1Δcth2Δ* cells displayed increased *ERG1* mRNA and protein levels, which is consistent with the negative effect of Cth1 and Cth2 proteins on *ERG1* expression (Figure 4A–C). The double mutant *cth1Δcth2Δ* grew similar to wild-type strain under both iron-sufficient and iron-deficient conditions (Figure S4A). Similar to *rox1Δ* cells and in accordance with Erg1 protein levels, *cth1Δcth2Δ* mutant

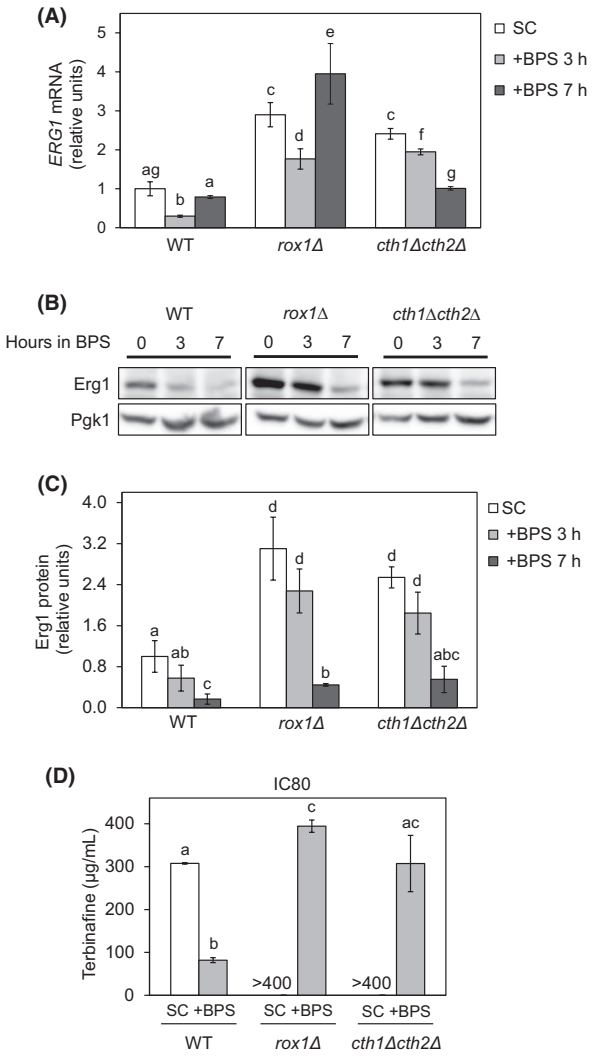

FIGURE 4 Deletion of *ROX1* or *CTH1/CTH2* increase Erg1 expression levels and terbinafine resistance. (A–C) Wild-type (WT, FY2609), *rox1Δ* and *cth1Δcth2Δ* strains were grown in SC medium as indicated in Figure 2. (A) *ERG1/ACT1* mRNA levels represented in relation to WT strain grown in SC are shown as the average of three biological samples. (B) Western blot image of Erg1 and Pgk1 protein levels of a representative experiment of three biological replicates. (C) Average and SD of the quantified Erg1/Pgk1 protein levels in relation to WT strain grown in SC. (D) *ROX1* and *CTH1/CTH2* deletion decreases terbinafine susceptibility. A terbinafine range from 3.12 to 400 μg/ml was tested at 28°C in media without (SC) or with 100 μM BPS (+BPS). Data show the average and SD of IC80 values of three biological replicates. Different letters above the bars represent statistically significant differences (p-value < 0.05).

exhibited a strongly reduced susceptibility to terbinafine (Figure 4D, S4B).

While Cth1 is expressed rapidly and transiently in response to iron depletion, Cth2 expression dramatically increases during the progress of iron limitation (Puig et al., 2005; Puig et al., 2008). To further test the Cth2-dependent regulation of *ERG1* mRNA upon iron deficiency, we expressed *CTH2* under the control of *TEF2* promoter (P_{TEF}-*CTH2*) in a *cth1Δcth2Δ* genetic background to remove any interference with the partially redundant Cth1 protein (Puig et al., 2008). As compared to cells expressing *CTH2* under its endogenous promoter (*CTH2*), the *TEF2* regulatory region enabled a strong expression of *CTH2* under iron-sufficient conditions (Figure 5A). Overexpression of *CTH2* (P_{TEF}-*CTH2* cells) led to a reduced expression of *ERG1* mRNA under iron replete conditions (Figure 5B). Consistent with mRNA levels, Erg1 protein abundance was decreased in P_{TEF}-*CTH2* cells under iron-sufficient conditions compared with wild-type cells (Figure 5C). The ectopic expression of *CTH2*, which barely slowed cell growth (Figure S5A), significantly increased terbinafine susceptibility under iron sufficiency (Figure 5D, S5B). The effect of P_{TEF}-*CTH2* expression on terbinafine susceptibility under iron-deficient conditions was not tested. In sum, these results indicate that Cth2 promotes the down-regulation of *ERG1*, thus becoming another important determinant of terbinafine susceptibility.

Effect of iron on Erg1 expression and terbinafine susceptibility in clinical and dietary *Saccharomyces cerevisiae* isolates

In recent years, *S. cerevisiae* has emerged as an opportunistic human fungal pathogen (Perez-Torrado & Querol, 2015; Wombwell et al., 2021). To assess the susceptibility of these strains to terbinafine and how iron bioavailability modulates it, we selected four *S. cerevisiae* strains from either clinical origin or isolated from dietary supplements, whose pathogenic potential has been previously reported (Clemons et al., 1994; de Llanos et al., 2004; de Llanos et al., 2006; de Llanos et al., 2011; Yañez et al., 2009). All the strains were cultivated in both iron-sufficient and iron-deficient media at 37°C, as this is the temperature that they are adapted to (Figure S6A, B). First, we checked the expression levels of Erg1 protein under iron-sufficient conditions in the different strains as compared with the laboratory strain BY4741. We observed that the clinical YJM128 strain (isolated from lung) and the dietetic D14 strain expressed higher basal levels of Erg1 than BY4147, the clinical D60 strain (isolated from vagina) and the dietetic Ultralevure strain (Figure 6A–C). To assess whether different basal levels of Erg1 protein were responsible for changes in terbinafine susceptibility, we checked terbinafine resistance in iron replete conditions (SC). We observed that BY4741 and D60 strains displayed similar terbinafine susceptibility and Erg1 levels (Figure 6A–D). YJM128 was the most terbinafine-resistant strain under iron replete conditions, probably due to its elevated Erg1 protein levels in SC as compared to the rest of strains analysed (Figure 6A–D). Despite D14 strain expressed high Erg1

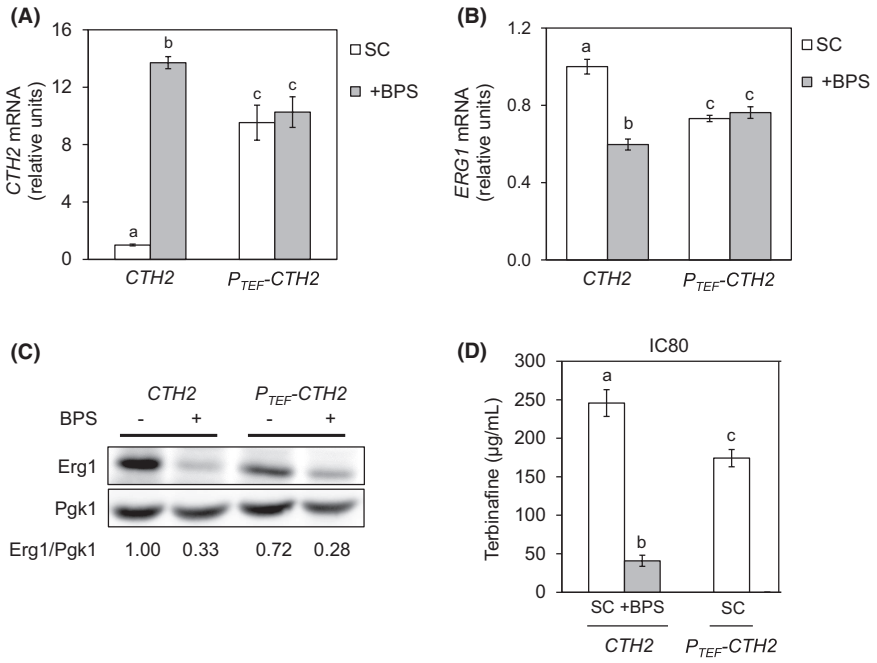

FIGURE 5 The overexpression of *CTH2* down-regulates *ERG1* and decreases terbinafine susceptibility. (A)–(C) Yeast BY4741 *cth1Δcth2Δ* cells transformed with pRS416-CTH2 (*CTH2*) or p416TEF-CTH2 (P_{TEF}-*CTH2*) were growth at 30°C for 6 h in SC-ura without (SC) or with 100 µM BPS (+BPS). (A)–(B) Average abundance of *CTH2* (A) and *ERG1* (B) transcripts normalized with *ACT1* of three biological replicates, represented in relation to *CTH2* cells grown in SC. (C) Western blot image of Erg1 and Pgk1 protein levels of a representative experiment of two biological samples. Numbers indicate Erg1/Pgk1 changes (n-fold) relative to WT strain in SC of that biological replica. (D) *CTH2*-overexpressing cells are more susceptible to terbinafine under iron-sufficient conditions. A terbinafine range from 3.12 to 400 µg/ml was tested at 28°C in media without (SC) or with 100 µM BPS (+BPS). Data show the average and SD of IC80 values of four biological replicates. Different letters above the bars represent statistically significant differences (p-value < 0.05).

levels under iron-sufficient conditions, it exhibited similar susceptibility to BY4741 and D60 (Figure 6A–D). Remarkably, Ultralevure was highly sensitive to terbinafine despite its Erg1 protein levels were similar to those of BY4741 and D60 strains (Figure 6A–D).

Then, we determined the effect of iron deprivation on Erg1 protein levels. Iron chelation limited the growth of all yeast strains, with D60 being the more resistant and YJM128 the more sensitive to iron depletion (Figure S6A, B). As in the laboratory strain BY4741, Erg1 protein rapidly decreased when yeast cells were iron deprived (Figure 6B–C). In accordance with the decreased Erg1 expression, iron starvation greatly increased terbinafine susceptibility of BY4741, YJM128 and D14 strains compared with iron replete conditions (Figure 6B–D, S6C–E). Regarding IC80 values, the enhanced susceptibility to terbinafine that iron chelation caused to D60 strain was very low and non-existent in Ultralevure strain (Figure 6D). However, a significant decrease in growth was observed for both strains when iron was chelated at lower concentrations of terbinafine (Figure S6F–G), as reflected by a reduction of IC50 values (Figure 6E). Altogether, these results indicate that Erg1 protein abundance decreases in iron-deficient conditions. In general, Erg1 downregulation by iron chelation causes an increase in terbinafine susceptibility, although the degree of susceptibility varies among the strains.

DISCUSSION

In this report, we analysed the expression pattern of yeast Erg1, which is the target of terbinafine, during the progress of iron deficiency. At the mRNA level, we observed an initial decrease (3 h) followed by a partial recovery of transcript levels (7 h) (Figure 1A). However, we observed that Erg1 protein levels decreased upon iron depletion, achieved by either chelating available iron or deleting the iron uptake factors *FET3* and *FET4* (Figure 1B and C). Previous studies have described a repression of bulk translation during adaptation to iron deficiency (Romero et al., 2019; Romero et al., 2020). Localization of *ERG1* transcript in ribosome profiles confirmed its translational repression upon iron limitation. *ERG1* mRNA peak moved from polysomal to monosomal fractions during the progress of iron starvation (Figure 1D). Additional studies have shown that iron deficiency limits the biosynthesis of ergosterol due to defects in specific enzymes that use iron as cofactor, leading to increased levels of the initial substrates, squalene and lanosterol (Jorda et al., 2021; Shakoury-Elizeh et al., 2010). To prevent the accumulation of free toxic sterol, lanosterol accumulation induces the degradation of Erg1 protein via the endoplasmic reticulum-associated protein degradation pathway (Foresti et al., 2013), which in turn has been described to be activated in response to iron deficiency

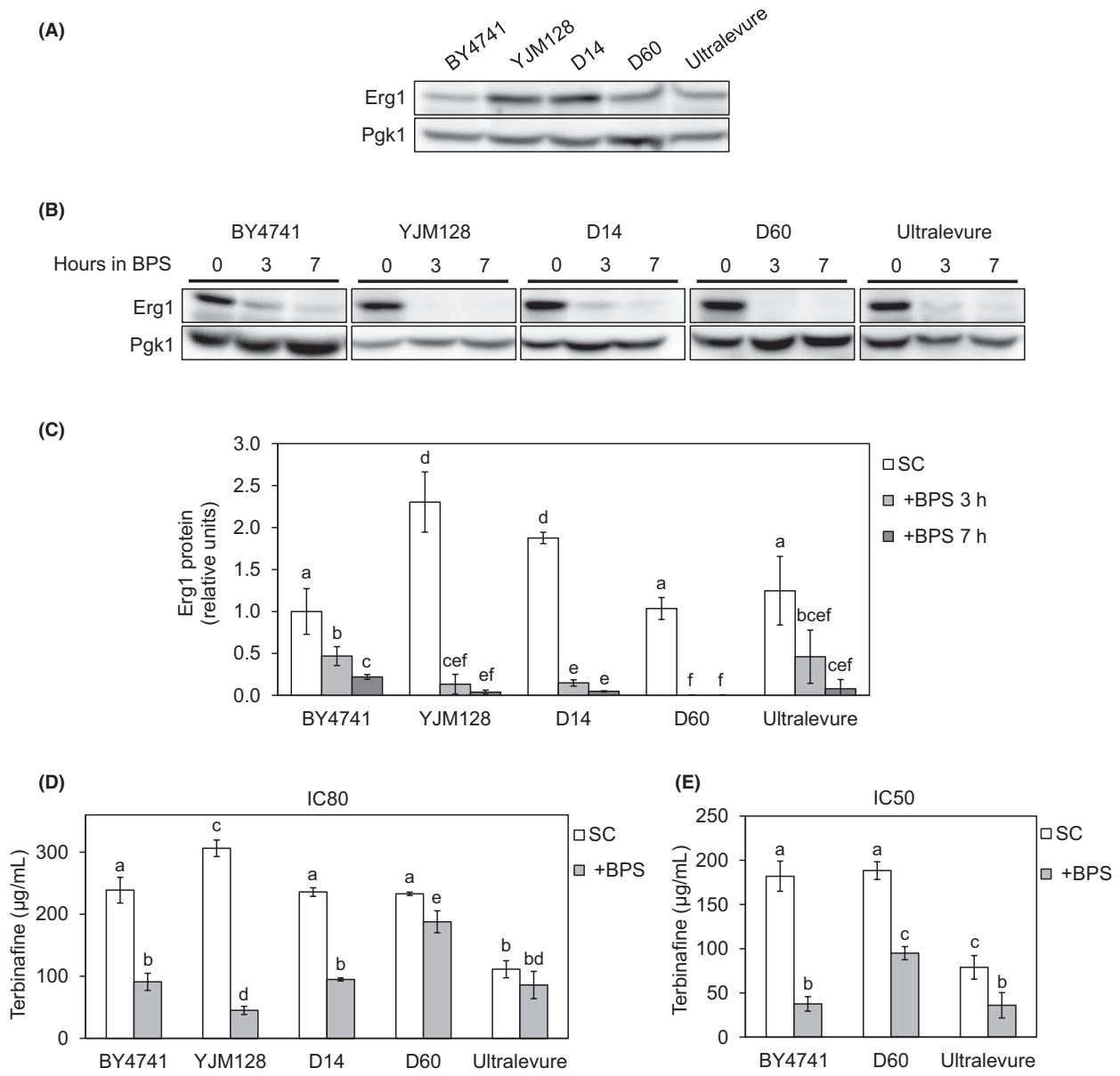

FIGURE 6 Iron deficiency affects Erg1 expression and terbinafine susceptibility in some potentially pathogenic *S. cerevisiae* strains. (A–C) Erg1 protein levels the laboratory *S. cerevisiae* strain BY4741, the YJM128 and D60 clinical isolates, and the D14 and Ultralevure food isolates cultivated in iron-sufficient and iron-deficient conditions. (A) A representative Western blot image of Erg1 and Pgk1 protein levels in exponentially growing cells cultivated in iron-sufficient conditions (SC) at 37°C is shown. (B) Erg1 protein levels decrease upon iron deficiency in clinical and dietary *S. cerevisiae* isolates. Yeast isolates were grown at 37°C in SC media as described in Figure 2. The protein levels of Erg1 and Pgk1 were analysed by Western blot as described in Materials and Methods. A representative experiment of at least two biological samples is shown. (C) Quantification of Erg1/Pgk1 protein levels for each strain during the progress of iron deficiency. Data show the average and SD of at least two biological replicates relative to each strain cultivated in SC. (D) Terbinafine susceptibility of the different *S. cerevisiae* isolates. A terbinafine range from 3.12 to 400 µg/ml was tested at 37°C in media without (SC) or with 100 µM BPS (+BPS). Data show the average and SD of IC80 values of three biological replicates. (E) IC50 values of the D60 and Ultralevure isolates strains in contrast to the BY4741 strains. The terbinafine concentrations that inhibited 50% of growth (IC50) were estimated as described in Materials and Methods. Different letters above the bars represent statistically significant differences (p-value < 0.05).

(Seo et al., 2008). These data strongly suggest that Erg1 protein is probably more unstable under iron deprivation conditions. Therefore, both a decrease in *ERG1* translation and a lanosterol-induced degradation of Erg1 may contribute to the drop of Erg1 abundance observed in iron-deficient yeasts. Consistent with a decrease in Erg1 levels, yeast cells displayed an enhanced sensitivity to terbinafine upon chemical or genetic iron deficiency that was rescued by ectopically overexpressing *ERG1* (Figures 1E, 2).

The DNA-binding protein Rox1 is responsible for the transcriptional repression of hypoxic genes and several ergosterol biosynthesis genes, including *ERG1*, under aerobic growth conditions (Jorda

& Puig, 2020). Previous studies have reported that deletion of *ROX1* results in increased *ERG1* expression and less susceptibility to terbinafine (Henry et al., 2002). Here, we show that *ROX1* deletion leads to an increase in *ERG1* transcript and protein levels under both iron-sufficient and iron-deficiency conditions (Figure 4), strongly suggesting that Rox1 also limits *ERG1* gene expression when iron bioavailability decreases. The regulation of *ERG* genes by Rox1 has just been reported to be conserved in the pathogen *Candida glabrata* (Ollinger et al., 2021). On the other hand, the mRNA-binding proteins Cth1 and Cth2 post-transcriptionally inhibit the expression of multiple ARE-containing mRNAs during adaptation to iron deficiency (Puig et al., 2005; Puig et al., 2008; Ramos-Alonso et al., 2018). Previous genome-wide studies have shown that *ERG1* transcript, which contains two putative AREs located 122 and 133 nucleotides downstream termination codon, is upregulated in iron-deficient yeast cells lacking Cth1 and Cth2 (Puig et al., 2008). Here, we show by RT-qPCR and Western blotting that indeed deletion of *CTH1* and *CTH2* increases Erg1 abundance (Figure 4). *CTH1*, which is expressed under normal conditions (Puig et al., 2008), may be limiting basal *ERG1* expression, whereas *CTH2*, which is only expressed upon iron depletion (Puig et al., 2005), may account for most *ERG1* downregulation in low iron conditions. Moreover, we show that *CTH2* constitutive expression under *TEF2* promoter causes the downregulation of Erg1 in iron-sufficient cells (Figure 5). These data indicate that Cth1 and Cth2 are negative regulators of *ERG1* expression. Consistent with upregulation in *ERG1* levels, yeast *rox1Δ* and *cth1Δcth2Δ* cells display an enhanced resistance to terbinafine (Figure 4D). On the contrary, overexpression of *CTH2* contributes to increase the sensitivity of yeast cells to terbinafine (Figure 5D). The regulatory role of Cth2 over iron metabolism has been recently confirmed in *C. glabrata* (Gerwien et al., 2016). These data indicate that Rox1 and Cth1/Cth2 proteins are potential targets to modulate yeast Erg1 protein levels and terbinafine sensibility in both iron replete and deficient conditions.

Despite the yeast *S. cerevisiae* is rarely pathogenic, various studies have reported infections of immunocompromised patients by particular clinical and dietetic strains of *S. cerevisiae* (Perez-Torrado & Querol, 2015; Wombwell et al., 2021). Here, we explored how iron modulates Erg1 protein levels and terbinafine susceptibility of various opportunistic *S. cerevisiae* strains. In general terms, we observed a correlation between Erg1 protein levels and terbinafine resistance. For instance, the clinical isolate YJM128, with the highest Erg1 expression levels, was the most terbinafine-resistant strain under normal growth conditions (Figure 6). Moreover, these strains diminished Erg1 expression and increased their susceptibility to terbinafine upon exposure to low iron conditions (Figure 6). Despite the general behaviour of these strains seemed similar to the laboratory BY4741 strain, some unexpected results were observed. Under low iron conditions, the probiotic Ultralevure exhibited similar terbinafine sensitivity and Erg1 protein levels to the laboratory strain. However, Ultralevure was highly susceptible to terbinafine under normal growth conditions, despite expressing Erg1 protein levels similar to those of the laboratory strain (Figure 6). Therefore, additional factors could contribute to different terbinafine sensitivity. (i) We have recently reported that mutants defective in ergosterol biosynthesis exhibit an impaired response to iron depletion due to mislocalization of the iron-responsive transcription factor Aft1 (Jorda et al., 2021). As iron depletion leads to profound changes in sterol composition (Jorda et al., 2021; Shakoury-Elizeh et al., 2010), we consider that the resulting problems in yeast adaptation to iron deficiency could also contribute to increase terbinafine susceptibility. We observed that YJM128 was the most terbinafine susceptible strain under iron-deficient conditions, probably because its growth is more severely affected by iron depletion than the rest of yeast strains (Figure 6, S6). On the contrary, D60 strain, which exhibited the most optimal growth in iron-depleted medium, displayed the highest terbinafine resistance (Figure 6, S6). (ii) Studies in *C. albicans* have described that iron depletion increases membrane fluidity and in turn facilitates the passive diffusion of drugs (Prasad et al., 2006), while changes in sterol composition by *ERG1* deletion reduces drug efflux due to a poor surface localization of the ATP-binding cassette (ABC) transporter Cdr1 (Pasrija et al., 2005). In *S. cerevisiae*, changes in sterol composition also disrupt the activity of efflux pumps, such as Pdr5 (Kodedova & Sychrova, 2015). In this sense, overexpression of *S. cerevisiae PDR5*, or its homologous *C. albicans CDR1* and *CDR2,* is associated with terbinafine resistance (Leber et al., 2003; Sanglard et al., 1997). Although a more detailed study is necessary, initial studies show different expression levels for *PDR5* in the natural *S. cerevisiae* strains analysed in this work (Figure S7). (iii) The differences observed between the potentially pathogenic strains tested here could be related to point changes in the *ERG1* coding or regulatory sequences, which are an important source of terbinafine resistance (Klobucnikova et al., 2003; Leber et al., 2003; Sagatova, 2021). Therefore, although a general correlation between iron bioavailability, Erg1 protein levels and terbinafine sensitivity can be stablished, other factors must be explored in particular cases.

This study with different strains of *S. cerevisiae* highlights the potential of using our knowledge of yeast iron metabolism to modulate *ERG1* expression to optimize terbinafine treatments. Beyond a few opportunistic strains, the large majority of *S. cerevisiae* strains lack the virulence factors that can be found in other

fungal pathogens. Thereby, the findings obtained with the model *S. cerevisiae* should be tested in the fungal pathogen under study.

ACKNOWLEDGEMENTS

We thank all the members of the Iron Homeostasis laboratory for technical assistance, and A. M. Romero for scientific discussion and their critical reading of the manuscript. We are also indebted to Dr. Chao-Wen Wang for Erg1 antibody, and Drs. Amparo Querol and Fred Winston for yeast strains used in this work.

CONFLICT OF INTEREST

The authors declare no financial or commercial conflict of interest.

DATA AVAILABILITY STATEMENT

The data that support the findings in this study are available from the corresponding author upon reasonable request.

ORCID

Sergi Puig https://orcid.org/0000-0002-1856-490X

REFERENCES

Arroyo-Lopez, F.N., Salvado, Z., Tronchoni, J., Guillamon, J.M., Barrio, E. & Querol, A. (2010) Susceptibility and resistance to ethanol in *Saccharomyces* strains isolated from wild and fermentative environments. *Yeast*, 27, 1005–1015.

Chua, N.K., Coates, H.W. & Brown, A.J. (2020) Squalene monooxygenase: a journey to the heart of cholesterol synthesis. *Progress in Lipid Research*, 79, 101033.

Clemons, K.V., McCusker, J.H., Davis, R.W. & Stevens, D.A. (1994) Comparative pathogenesis of clinical and nonclinical isolates of *Saccharomyces cerevisiae*. *The Journal of Infectious Diseases*, 169, 859–867.

Clinical and Laboratory Standards Institute. (2008) Reference method for broth dilution antifungal susceptibility testing of yeasts. In: *CLSI standard M27-A3 (28)*, 3rd edition. Wayne, PA USA: Clinical and Laboratory Standards Institute.

de Llanos, R., Fernandez-Espinar, M.T. & Querol, A. (2006) A comparison of clinical and food *Saccharomyces cerevisiae* isolates on the basis of potential virulence factors. *Antonie Van Leeuwenhoek*, 90, 221–231.

de Llanos, R., Llopis, S., Molero, G., Querol, A., Gil, C. & Fernandez-Espinar, M.T. (2011) In vivo virulence of commercial *Saccharomyces cerevisiae* strains with pathogenicity-associated phenotypical traits. *International Journal of Food Microbiology*, 144, 393–399.

de Llanos, R., Querol, A., Planes, A.M. & Fernandez-Espinar, M.T. (2004) Molecular characterization of clinical *Saccharomyces cerevisiae* isolates and their association with non-clinical strains. *Systematic and Applied Microbiology*, 27, 427–435.

Demuyser, L. & Van Dijck, P. (2019) Can *Saccharomyces cerevisiae* keep up as a model system in fungal azole susceptibility research? *Drug Resistance Updates*, 42, 22–34.

Fisher, M.C., Hawkins, N.J., Sanglard, D. & Gurr, S.J. (2018) Worldwide emergence of resistance to antifungal drugs challenges human health and food security. *Science*, 360, 739–742.

Foresti, O., Ruggiano, A., Hannibal-Bach, H.K., Ejsing, C.S. & Carvalho, P. (2013) Sterol homeostasis requires regulated degradation of squalene monooxygenase by the ubiquitin ligase Doa10/Teb4. *Elife*, 2, e00953.

Gerwien, F., Safyan, A., Wisgott, S., Hille, F., Kaemmer, P., Linde, J. et al. (2016) A novel hybrid iron regulation network combines features from pathogenic and nonpathogenic yeasts. *mBio*, 7, e01782.

Gnat, S., Lagowski, D. & Nowakiewicz, A. (2020) Major challenges and perspectives in the diagnostics and treatment of dermatophyte infections. *Journal of Applied Microbiology*, 129, 212–232.

Hausmann, A., Samans, B., Lill, R. & Muhlenhoff, U. (2008) Cellular and mitochondrial remodeling upon defects in iron-sulfur protein biogenesis. *The Journal of Biological Chemistry*, 283, 8318–8330.

Henry, K.W., Nickels, J.T. & Edlind, T.D. (2002) ROX1 and ERG regulation in *Saccharomyces cerevisiae*: implications for antifungal susceptibility. *Eukaryotic Cell*, 1, 1041–1044.

Hosogaya, N., Miyazaki, T., Nagi, M., Tanabe, K., Minematsu, A., Nagayoshi, Y. et al. (2013) The heme-binding protein Dap1 links iron homeostasis to azole resistance via the P450 protein Erg11 in Candida glabrata. *FEMS Yeast Research*, 13, 411–421.

Jorda, T. & Puig, S. (2020) Regulation of ergosterol biosynthesis in *Saccharomyces cerevisiae*. *Genes (Basel)*, 11, 795.

Jorda, T., Rozes, N. & Puig, S. (2021) Sterol composition modulates the response of *Saccharomyces cerevisiae* to iron deficiency. *J Fungi (Basel)*, 7, 901.

Klobucnikova, V., Kohut, P., Leber, R., Fuchsbichler, S., Schweighofer, N., Turnowsky, F. et al. (2003) Terbinafine resistance in a pleiotropic yeast mutant is caused by a single point mutation in the ERG1 gene. *Biochemical and Biophysical Research Communications*, 309, 666–671.

Kodedova, M. & Sychrova, H. (2015) Changes in the sterol composition of the plasma membrane affect membrane potential, salt tolerance and the activity of multidrug resistance pumps in *Saccharomyces cerevisiae*. *PLoS One*, 10, e0139306.

Kushnirov, V.V. (2000) Rapid and reliable protein extraction from yeast. *Yeast*, 16, 857–860.

Lai, Y.W., Campbell, L.T., Wilkins, M.R., Pang, C.N., Chen, S. & Carter, D.A. (2016) Synergy and antagonism between iron chelators and antifungal drugs in Cryptococcus. *International Journal of Antimicrobial Agents*, 48, 388–394.

Leber, R., Fuchsbichler, S., Klobucnikova, V., Schweighofer, N., Pitters, E., Wohlfarter, K. et al. (2003) Molecular mechanism of terbinafine resistance in *Saccharomyces cerevisiae*. *Antimicrobial Agents and Chemotherapy*, 47, 3890–3900.

Leber, R., Zenz, R., Schrottner, K., Fuchsbichler, S., Puhringer, B. & Turnowsky, F. (2001) A novel sequence element is involved in the transcriptional regulation of expression of the ERG1 (squalene epoxidase) gene in *Saccharomyces cerevisiae*. *European Journal of Biochemistry*, 268, 914–924.

Llopis, S., Hernandez-Haro, C., Monteoliva, L., Querol, A., Molina, M. & Fernandez-Espinar, M.T. (2014) Pathogenic potential of Saccharomyces strains isolated from dietary supplements. *PLoS One*, 9, e98094.

Martinez-Pastor, M.T. & Puig, S. (2020) Adaptation to iron deficiency in human pathogenic fungi. *Biochimica et Biophysica Acta. Molecular Cell Research*, 1867, 118797.

Monk, B.C., Sagatova, A.A., Hosseini, P., Ruma, Y.N., Wilson, R.K. & Keniya, M.V. (2020) Fungal Lanosterol 14alpha-demethylase: a target for next-generation antifungal design. *Biochimica et Biophysica Acta. Proteins and Proteomics*, 1868, 140206.

Ollinger, T.L., Vu, B., Murante, D., Parker, J.E., Simonicova, L., Doorley, L., et al. (2021) Loss-of-function ROX1 mutations suppress the fluconazole susceptibility of upc2AΔ mutation in Candida glabrata, implicating additional positive regulators of ergosterol biosynthesis, bioRxiv.

Pasrija, R., Krishnamurthy, S., Prasad, T., Ernst, J.F. & Prasad, R. (2005) Squalene epoxidase encoded by ERG1 affects morphogenesis and drug susceptibilities of *Candida albicans*. *The Journal of Antimicrobial Chemotherapy*, 55, 905–913.

Pedro-Segura, E., Vergara, S.V., Rodriguez-Navarro, S., Parker, R., Thiele, D.J. & Puig, S. (2008) The Cth2 ARE-binding protein

recruits the Dhh1 helicase to promote the decay of succinate dehydrogenase SDH4 mRNA in response to iron deficiency. *The Journal of Biological Chemistry*, 283, 28527–28535.
Perez-Torrado, R. & Querol, A. (2015) Opportunistic strains of *Saccharomyces cerevisiae*: a potential risk sold in food products. *Frontiers in Microbiology*, 6, 1522.
Pfaffl, M.W., Horgan, G.W. & Dempfle, L. (2002) Relative expression software tool (REST) for group-wise comparison and statistical analysis of relative expression results in real-time PCR. *Nucleic Acids Research*, 30, e36.
Prasad, T., Chandra, A., Mukhopadhyay, C.K. & Prasad, R. (2006) Unexpected link between iron and drug resistance of Candida spp.: iron depletion enhances membrane fluidity and drug diffusion, leading to drug-susceptible cells. *Antimicrobial Agents and Chemotherapy*, 50, 3597–3606.
Puig, S., Askeland, E. & Thiele, D.J. (2005) Coordinated remodeling of cellular metabolism during iron deficiency through targeted mRNA degradation. *Cell*, 120, 99–110.
Puig, S., Vergara, S.V. & Thiele, D.J. (2008) Cooperation of two mRNA-binding proteins drives metabolic adaptation to iron deficiency. *Cell Metabolism*, 7, 555–564.
Ramos-Alonso, L., Romero, A.M., Soler, M.A., Perea-Garcia, A., Alepuz, P., Puig, S. et al. (2018) Yeast Cth2 protein represses the translation of ARE-containing mRNAs in response to iron deficiency. *PLoS Genetics*, 14, e1007476.
Romero, A.M., Ramos-Alonso, L., Alepuz, P., Puig, S. & Martinez-Pastor, M.T. (2020) Global translational repression induced by iron deficiency in yeast depends on the Gcn2/eIF2alpha pathway. *Scientific Reports*, 10, 233.
Romero, A.M., Ramos-Alonso, L., Montella-Manuel, S., Garcia-Martinez, J., de la Torre-Ruiz, M.A., Perez-Ortin, J.E. et al. (2019) A genome-wide transcriptional study reveals that iron deficiency inhibits the yeast TORC1 pathway. *Biochimica et Biophysica Acta. Gene Regulatory Mechanisms*, 1862, 194414.
Ryder, N.S. (1992) Terbinafine: mode of action and properties of the squalene epoxidase inhibition. *The British Journal of Dermatology*, 126(Suppl 39), 2–7.
Ryder, N.S., Wagner, S. & Leitner, I. (1998) In vitro activities of terbinafine against cutaneous isolates of Candida albicans and other pathogenic yeasts. *Antimicrobial Agents and Chemotherapy*, 42, 1057–1061.
Sagatova, A.A. (2021) Strategies to better target fungal squalene monooxygenase. *Journal of Fungi (Basel)*, 7, 49.
Sanglard, D., Ischer, F., Monod, M. & Bille, J. (1997) Cloning of Candida albicans genes conferring resistance to azole antifungal agents: characterization of CDR2, a new multidrug ABC transporter gene. *Microbiology (Reading)*, 143(Pt 2), 405–416.
Sanvisens, N., Romero, A.M., An, X., Zhang, C., de Llanos, R., Martinez-Pastor, M.T. et al. (2014) Yeast Dun1 kinase regulates ribonucleotide reductase inhibitor Sml1 in response to iron deficiency. *Molecular and Cellular Biology*, 34, 3259–3271.
Seo, H.Y., Chang, Y.J., Chung, Y.J. & Kim, K.S. (2008) Proteomic analysis of recombinant *Saccharomyces cerevisiae* upon iron deficiency induced via human H-ferritin production. *Journal of Microbiology and Biotechnology*, 18, 1368–1376.
Shakoury-Elizeh, M., Protchenko, O., Berger, A., Cox, J., Gable, K., Dunn, T.M. et al. (2010) Metabolic response to iron deficiency in *Saccharomyces cerevisiae*. *The Journal of Biological Chemistry*, 285, 14823–14833.
Singh, P. (2016) Budding yeast: an ideal backdrop for in vivo lipid biochemistry. *Frontiers in Cell and Development Biology*, 4, 156.
Wombwell, E., Bransteitter, B. & Gillen, L.R. (2021) Incidence of *Saccharomyces cerevisiae* fungemia in hospitalised patients administered Saccharomyces boulardii probiotic. *Mycoses*, 64, 1521–1526.
Yañez, A., Murciano, C., Llopis, S., Fernández-Espinar, T., Gil, M.L. & Gozalbo, D. (2009) In vivo and in vitro studies on virulence and host responses to *Saccharomyces cerevisiae* clinical and non-clinical isolates. *The Open Mycology Journal*, 3, 37–47.

SUPPORTING INFORMATION

Additional supporting information can be found online in the Supporting Information section at the end of this article.

How to cite this article: Jordá, T., Martínez-Martín, A., Martínez-Pastor, M.T. & Puig, S. (2022) Modulation of yeast Erg1 expression and terbinafine susceptibility by iron bioavailability. *Microbial Biotechnology*, 15, 2705–2716. Available from: https://doi.org/10.1111/1751-7915.14102